Experimental investigation of counter current air-water flow in a large diameter vertical pipe with inners

2014 J. Phys.: Conf. Ser. 547 012024

(http://iopscience.iop.org/1742-6596/547/1/012024)

Journal of Physics: Conference Series **547** (2014) 012024 doi:10.1088/1742-6596/547/1/012024

Experimental investigation of counter current air-water flow in a large diameter vertical pipe with inners

Giorgio Besagni, Gaël Guédon, Fabio Inzoli
Politecnico di Milano, Department of Energy, Via Lambruschini 4a, 20156, Milano

E-mail: giorgio.besagni@polimi.it

Abstract. Counter current two phase flow is encountered in a wide variety of industrial applications. This paper describes the experimental results obtained in a circular column of 240 mm diameter with two inner pipes. The counter current flow studied concerns an upward flow of air and a downward flow of water at ambient temperature and pressure. The following range of operating conditions was analysed: superficial air velocities up to 23 cm/s and superficial water velocities up to - 11 cm/s, corresponding to a global air volume fractions (gas holdup) up to 29%. The experimental investigation concerned (i) flow visualization, (ii) local data from a double fibre optical probe and (iii) gas holdup measurements. The images obtained from an optical camera were used to observe the general flow patterns. The data obtained from the double fibre optical probe were used to study the local flow characteristics. In particular, the local void fractions, the bubble velocities, the bubble mean diameters and the bubble diameter distributions and are presented and discussed. The bed expansion technique was used to obtain the gas holdup measurements for every operating condition. The gas holdup measurements are discussed, compared with existing correlations and used for investigating the flow regime transitions. Finally, the gas holdup and the local void fraction measurements data are compared and used for understanding the local hydrodynamics.

1. Introduction

Two-phase flow in vertical pipes is encountered in several plants in the chemical and in the nuclear fields. The chemical industries utilize vertical pipes in bubble columns and in fluidized beds for heat and mass transfer operations. In the nuclear industry, a typical example of vertical pipe is the natural circulating flow in the chimney region of Boiling Water Reactor (BWR). The correct design and operation of these devices can be managed with the proper prediction of the flow patterns and flow properties at the operating conditions of interest. These information can be obtained by using experimental investigations. In the broader framework of two phase flow in vertical pipes, we focus on counter current air-water flow in a large diameter vertical pipe.

Two-phase vertical counter-current flow has been investigated experimentally by several researchers using intrusive and non-intrusive techniques. Yamaguchi and Yasaburo [1] investigated cross-sectional void fractions of co-current and counter current air–water flow in vertical pipes with inner diameters of 40 and 80 mm. The cross-sectional void fraction was measured by a quick-closing valve method. These experiments were carried out in bubbly and slug flow regimes. Hasan et al. [2] investigated cross-sectional void fractions of air–water co-current and counter current flow in a vertical pipe with an inner diameter of 127 mm. The cross-sectional void fraction was calculated using a pressure drop technique. These experiments were carried out in bubbly and slug flow regimes. Aritomi et al. [3-5] investigated the behaviours of counter current flow in a rectangular channel. Local

void fraction was measured by an ultrasonic technique. These experiments were carried out in bubbly flow regime. Fuangworawong et al. [6] investigated local void fractions of air–water counter current flow in a vertical pipe with an inner diameter of 50 mm. The local void fractions were calculated using a wire mesh tomography technique. These experiments were carried out in bubbly flow regime. Ghosh et al. [7, 8] investigated cross-sectional void fractions of air–water counter current flow in a vertical pipe with an inner diameter of 26.4 mm. The cross-sectional void fractions were calculated using a wire conductivity probe technique. These experiments were carried out in slug, churn and annular regimes, including the flooding condition.

All the previous studies were focused on small diameter pipes. The present investigation concerns a pipe with inner diameter of 240 mm, which is a large diameter pipe under the ambient operating conditions. The size range of a pipe is determined by the non-dimensional hydraulic diameter D^*_H [9]:

$$D_H^* = \frac{D_H}{\sqrt{\sigma / g\left(\rho_l - \rho_g\right)}} \tag{1}$$

where D_H is the hydraulic diameter, σ is the surface tension, g is the force due to gravity and ρ_l-ρ_g is the density difference between the phases. Pipes with non-dimensional diameters greater than a critical (or transitional) value $D^*_{H,cr}$ are considered to be large diameter pipes. The critical value is reported to be $D^*_{H,cr}$ = 52 [10]. The above critical diameter corresponds to $D_H \approx$ 130 mm for air and water at atmospheric conditions and $D_H \approx$ 63 mm for BWR operating conditions. The critical value $D^*_{H,cr}$ is given in terms of the Taylor wavelength. When the pipe diameter is larger than such a value, the stabilizing effect of the channel wall on the interface of the Taylor bubbles become lower and Taylor bubble can no longer be sustained due to the Raleigh–Taylor instability. The interaction of these two instabilities results in large bubbles being broken into many smaller cap-shaped bubbles. Hence, large diameter pipes can be defined as flow channels in which stable slug bubbles cannot be sustained [9]. The above-mentioned studies have a non-dimensional diameter of D^*_H = 14.69 – 29.38 [1], 46.64 [2], 18.18 [3-5], 18.38 [6] and 9.69 [7.8]. All of these values are below the critical value of 52. Indeed in these studies the slug flow is reported and/or can exist. This is particularly interesting for [2], which has a non-dimensional diameter D^*_H = 46.64. This pipe can be considered as an intermediate pipe. Indeed, the values is a little bit below the critical value (indeed, the slug flow appears). Generally speaking, flow in large pipes has several significant differences from flow in small pipes because of the many changes to the hydrodynamics: change in bubble drag, presence of additional turbulence [11] and strong secondary recirculation in the flow. The three-dimensional circulatory behaviour is due to the liquid flowing around the cap bubbles rather than being forced out of the way, as is the case with slug bubbles. These changes result in very different physical mechanisms behind the transport of gas and liquid and causes significant changes to the void fraction and velocity profiles flow in smaller pipes. Indeed, turbulence, along with the lift, turbulent dispersion and the wall lubrication force, plays an important role in determining the void profiles [12] and can also result in enhanced bubble breakup. It should be noted that these differences may become less significant for higher liquid velocities where the turbulent intensity is already very high [13]. For all these reasons, the models typically used to predict the behaviour of two-phase flow in small diameter pipes, in which slug flow exists, may not be scaled for use in understanding flow in large diameter pipes [14]. Furthermore, flow regime maps and criteria to determine flow regime transitions for large pipes differs from small diameter ones [15, 16].

Even with the several progresses made in the field of two-phase flow, there is still little knowledge of counter-current flow in large diameter pipes. In addition, studies involving also the presence of inner pipes are rare [17] and are focused on a small diameter pipe. Moreover, we focus on a layout never studied in the literature. For the above mentioned reasons, experimental data and correlations must be specifically developed for the analysis of this system. The present study is aimed at providing insights into such flow configuration through an experimental investigation. The following range of operating conditions was analysed: superficial air velocities up to 23 cm/s and superficial water velocities up to -11 cm/s, corresponding to global air volume fractions (holdup) up to 29%. The experimental investigations concerned (i) flow visualization, (ii) local data from a double optical probe and (iii)

holdup measurements. Images obtained from an optical camera were used to observe the general flow pattern. Data obtained from the double optical probe were used to study local flow characteristics. In particular, the local void fractions, the bubble velocities, the bubble mean diameters and the bubble diameter distributions and are presented and discussed. The bed expansion technique was used to obtain the gas holdup measurements for every operating condition. The gas holdup measurements are discussed, compared with existing correlations and used for investigating flow regime transition. Finally, the gas holdup and the local void fraction measurements are compared and used for understanding the local hydrodynamics.

2. Experimental setup

The experimental facility (figure 1) consists of a non-pressurised vertical pipe made of Plexiglas with d_{column} = 240 mm and H_{column} = 5.3 m. An internal pipe, made of PVC, with an external diameter of 60 mm, is centrally positioned, while another internal pipe, also made of PVC, with an external diameter of 75 mm, is positioned asymmetrically. A pump, controlled by a by-pass valve, provides water recirculation. A rotameter (3) measures the water flow rate. A pressure redactor controls the pressure upstream the rotameters (1) and (2), used to measure the air flow rate. The air distributor, which is positioned asymmetrically, is made of a stainless steel tube with an external diameter of 70 mm, an height of 340 mm and has holes positioned along the circumference. Various hole diameters ranging from d_{holes} = 1 mm to d_{holes} = 5 mm were investigated and it was found that the hole diameter has no influence on the bubble Sauter mean diameter (measured in the flow developed region). In this study, a distributor with d_{holes} = 3.5 mm is used. Due to the nature of the observed flow phenomena and their sensitivity to surface tension forces, clean filtered deionized water was used. Furthermore, the system was flushed beforehand for long periods of time to remove contaminants. During the experiments, the air was maintained at atmospheric pressure at the outlet of the test section, and the air and water temperatures were maintained constant. At the start of each test, the water height is set to z = 3.245 m. In this study, the values of gas density and superficial gas velocity are based upon the operating conditions existing at the column mid-point, such as suggested by [18]. The mid-point column pressure, used to compute gas density, was assumed to be equal to the column outlet pressure plus one-half the total experimental hydrostatic pressure head.

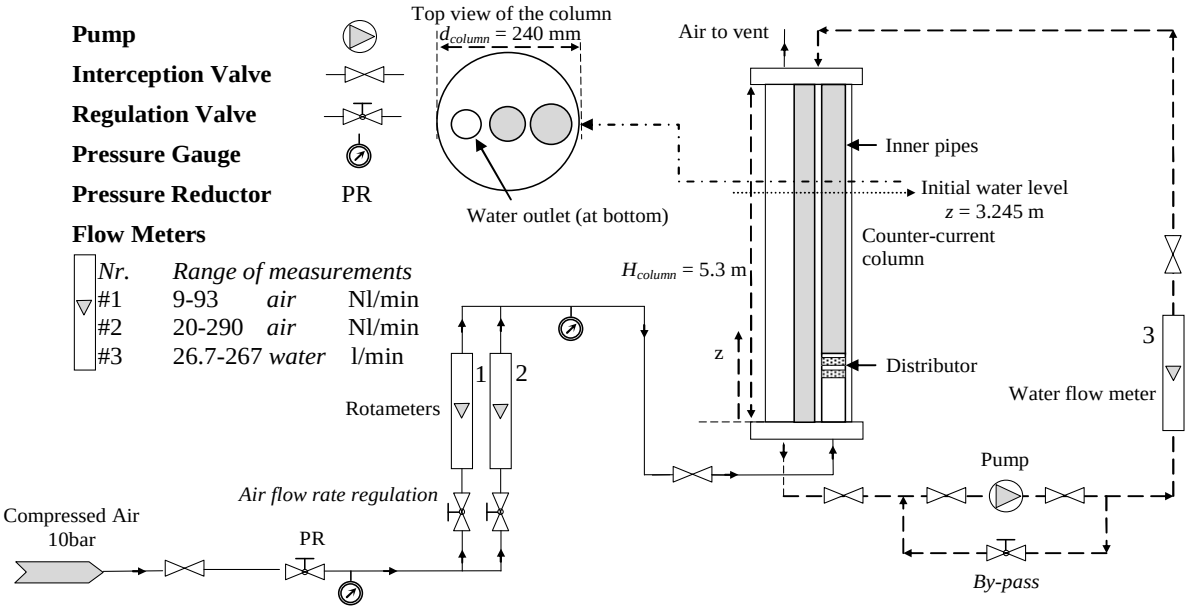

Figure 1. Experimental facility.

3. Measurement techniques

The local bubble properties were measured using a double fibre optical probe. The gas holdup measurements were determined using the bed expansion technique. Photos were taken at selected conditions. All the measurements were taken after the system reached the steady state.

3.1. Local measurements

Local flow properties have been measured by means of a double fibre optical probe system [19] manufactured by RBI (France). The optical probe is inserted, via an access port (figure 2), into the flow at a height of z = 2.3 m from the bottom (z = 1.9 m from the air distributor). Optical probes are intrusive phase detection tools that distinguish the gas and liquid phases by measuring the intensity of a laser light that is reflected at the probe tip when submerged in either phase. The laser is reflected and/or refracted at varying intensities depending on the probe tip geometry and the refractive indexes of the probe tip ($n_{tip} \approx 1.6$), gas ($n_{air} \approx 1$), and liquid ($n_{water} \approx 1.33$) phases. The probe signal is measured via an optoelectronic module which emits the laser to the probe tip and converts the reflected optical signal into a digital signal. The resulting signal distinguishes between the gas and the liquid phases. The response time of the cell is 0.5–1 μs, thus local phase interfaces are detected instantaneously. The time averaged local flow properties measured are the local void fraction, bubble vertical velocity, bubble size, interfacial area concentration and bubble chord length distributions. All the acquisitions are performed using a sampling period equal to $\Delta t_{sampling}$ = 1000 s. This measurement period is large enough to produce reliable time-averaged values. However, there are some potential sources of errors when characterizing bubbles using optical probes. Among the various effects we may state: (i) the improper dewetting at the probe tip (the blinding effect), (ii) the alteration of bubble trajectory prior to or during the piercing process (the drifting effect) and (iii) bubble deformation and/or deceleration at the probe tip (the crawling effect) [19, 20].

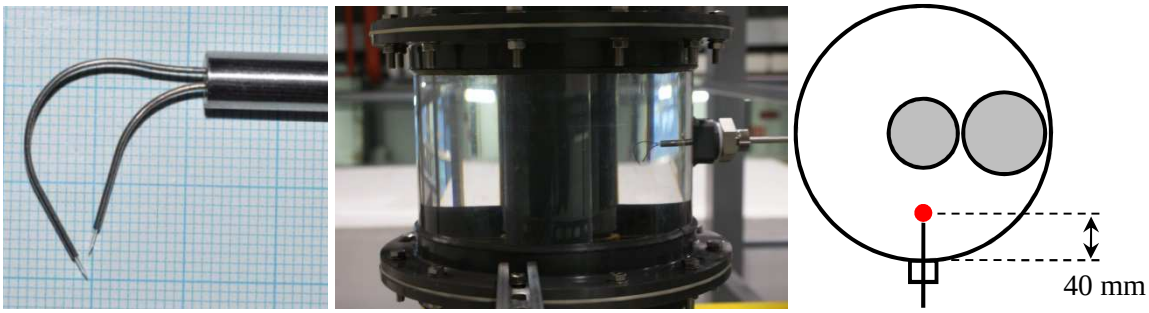

Figure 2. The double fibre optical probe and its position within the pipe cross-section.

3.2. Holdup measurements

Measurements of the bed expansion allowed the evaluation of the global void fraction ε_{air} (gas holdup). The procedure involves measuring the change of liquid height when air is introduced in the column. The global void fraction is then obtained using:

$$\varepsilon_{air} = \left(H_D - H_0\right) / H_D \qquad (2)$$

where H_D and H_0 are the heights of the free-surface after and before aeration, respectively. The change in liquid height is measured after a steady averaged liquid level is reached. The “holdup” and the “global void fraction” have the same meaning and refer to the same definition, the equation (2).

3.3. Photography

Photos were taken using a Canon α200 camera (1/1000s, ISO400). The back light method is employed in the experiments and the light source is provided by a 500 W halogen lamp. Visualization sections consist in squared boxes (filled with water) around the vertical pipe for correcting the distorted image. The camera was aligned horizontally to the visualization sections.

4. Results

4.1. Flow regimes description and discussion

4.1.1. Flow regime description

Ranging from low to high superficial gas velocity we have observed the homogeneous-bubbly and the heterogeneous-churn turbulent flow regime, with a transition zone between the two regimes. We have not observed a stable slug flow, the annular flow and the flooding condition. Qualitatively speaking, for low air superficial velocities, bubbly flow is observed (figure 3). In this regime, bubbles are uniformly distributed in the cross section of the pipe, traveling vertically with minor transverse and axial oscillations. Bubbles have not a regular spherical shape. Around the inner pipes we have observed bubble recirculation and the periodic appearance of cap-bubbles. The cap-bubbles seem to originate because of the bubble coalescence around the inner pipes. Due to the presence of these cap-bubbles this regime can be better defined as a pseudo-homogeneous regime. Increasing air flow rate, we have observed a transition zone (figure 4) toward the heterogeneous regime (figure 5). Here, we have noticed an increased coalescence rate. Finally, a fully developed churn turbulent regime is reached (figure 6). In this condition we have observed periodic very large bubble which occupy the major part of the cross section of the pipe. Those bubbles stake the form of spherical caps with a very mobile and flexible interface. Increasing the water flow rate, we have observed an increase in bubble number, a reduced bubble rising velocity and highly recirculating phenomena.

Figure 3. J_{air} = 0.87 cm/s– J_{water} = 0 cm/s.

Figure 4. J_{air} = 4.09 cm/s – J_{water} = 0 cm/s.

Figure 5. J_{air} = 11.94 cm/s – J_{water} = 0 cm/s.

Figure 6. J_{air} = 19.91 cm/s – J_{water} = 0 cm/s.

4.1.2. Flow regime discussion

Flow regimes can be discussed with three main considerations: (i) counter current flow, (ii) large diameter pipe and (iii) the presence of inner pipes. Firstly, the two-phase flow dynamics in the counter-current flow configuration is very similar to the bubble column configuration. Large periodic eddies accompanied with flow recirculation are observed all along the vertical development of the

pipe. Secondly, flow phenomena can be detailed with reference to large diameter pipe theory. In the present case, the dimensionless diameter is D^*_H = 88.13, if the inner pipes are not considered, and D^*_H = 47.37, if the inner pipes are considered. The former value if above the critical value of 52 [10] and the latter is below. Hence, we are studying an intermediate pipe that originates from a large diameter pipe. This explains the absence of a fully developed stable slug regime and the existence of periodic very large bubbles which occupies a large part of the pipe. Stable Taylor bubble has not been detected. Taylor bubbles were noticed only when the air flowmeters were opened and air was introduced in the pipe with stagnant water. After this occurrence stable Taylor bubbles could no more exist because of the turbulence in the pipe and the above-discussed instabilities. Moreover, in a large diameter pipe, high turbulence is expected and, in the present case, the turbulence intensity is such that bubble coalescence and break-up constantly occur even at low gas flow rate. The high flow mixing is the reason why the flow field rapidly becomes developed: distance of about 5÷7 d_{inner} is required for the flow to develop downstream the air distributor. Accordingly, the double optical probe measurements are taken at z = 1.9 m ≈ 8 d_{inner} from the air distributor. Thirdly, the presence of inner pipes may influence the flow characteristics. At first, cap-bubbles are noticed to originate along the inner pipes. At second they may provide additional recirculating flow phenomena, affecting the turbulence intensity and the size and frequency of the turbulent eddies. The presence of additional turbulence is verified in the present experiments: an analysis of different distributor hole diameters and configurations did not influenced the flow dynamics and bubble sauter mean diameters.

4.2. Gas holdup measurements and flow regime transitions

4.2.1. Gas holdup

The gas holdup data has been measured for superficial air velocities up to 23 cm/s and superficial water velocities up to - 11 cm/s (figure 7, left). At low air superficial, the relation between the gas holdup and the superficial gas velocity is linear, followed by a change in tendency at a certain transition superficial gas velocity. The linear trend corresponds to bubbly flow and the change in tendency is due to flow regime transition toward the bubbly-churn transition zone. Indeed, in dispersed flow and assuming proper gas distribution, gas holdup increases linearly as a function of the gas flow rate, where more bubbles of similar size occupy more volume in the column. Increasing the superficial water velocity, the holdup increase because bubble rise velocity decrease. Above the transition velocity, bubble coalescence increases the average rise velocity (figure 9) and reduces gas residence time in the column, hence decreasing the gas holdup versus gas velocity slope. From flow visualisations, a progressive change in flow regime is observed in correspondence to this phenomenon, i.e., the flow turbulence starts to increase significantly and large deformed bubbles starts to appear. The transition toward the heterogeneous regime is completed at about ε_{air} ≈ 16%. Above ε_{air} ≈ 16-17 %, another phenomenon is identified when the counter-current flow configuration is considered: the water superficial velocity has no influence on the gas holdup. The non-influence of water velocity on the gas holdup is a matter of further investigation. Here, we propose two possible explanations for this phenomena. The first explanation concerns the role of the turbulence. The two-phase flow dynamics is mainly dominated by turbulence in large diameter pipes. Moreover, it is known from the literature that, for high liquid velocities, when the turbulence intensity is already high, the discrepancies in the fluid dynamics become less significant [13]. The second explanation concerns the distribution of the phases in the column. At such conditions large bubbles, that occupies the major part of the cross section of the pipes, appears and the liquid is mainly concentrated along the wall pipe. These hypotheses can be validated only performing investigation without the presence of the inner pipes. The reported void fraction trend can be justified by considering the contribution of small and large bubbles [21]. In the churn-turbulent flow regime, the contribution of small bubbles to overall holdup is constant, whereas the large bubble holdup increases with increasing superficial velocity. On the contrary, in bubbly flow, small bubble holdup is not constant but changes significantly as the superficial velocity is changed.

4.2.2. Flow regime transition

The flow regime transition description proposed in the previous paragraph is here supported using a more quantitative analysis. In particular, the flow regime transition from bubbly flow to the transition zone can be predicted using the method proposed by Krishna et al. [22] by plotting the swarm rise velocity (defined as the ratio of superficial gas velocity to gas holdup) versus corresponding superficial gas velocity (figure 7, right). The swarm velocity was found to be constant in the homogeneous regime, but it starts to increase as the system enters the heterogeneous regime at a certain transition superficial velocity. The transition velocity decreases while increasing the superficial liquid velocity. The appearance of the first large bubble is responsible for such sudden increase in swarm velocity and is an indication of flow regime transition. Further investigations concerning flow regime transition are matter of future works.

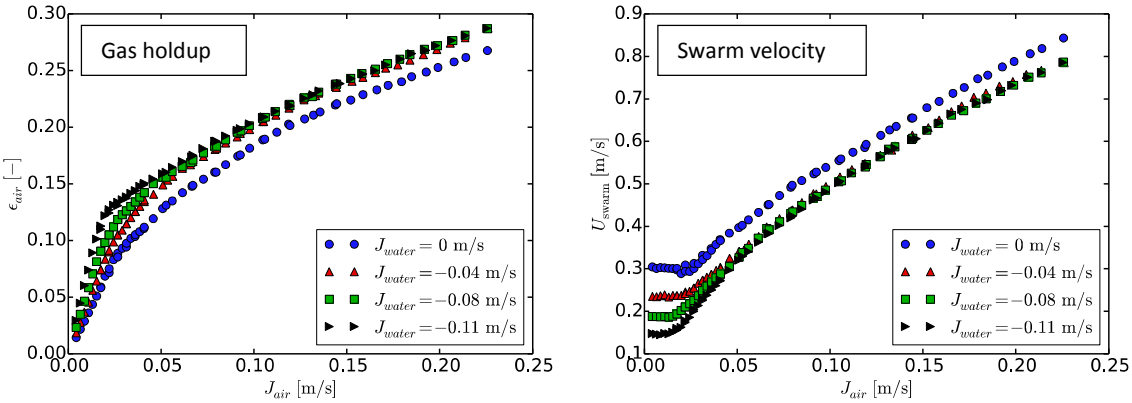

Figure 7. Gas holdup measurements (left) and swarm velocity (right).

4.2.3. Comparison with correlation

The data taken in the bubble column configuration (J_{water} = 0 cm/s) are compared (figure 8) with four correlations for the holdup prediction in bubble column reactors: Reilly et al. [23], Joshi and Sharma [24], Hughmark [25] the Kawase and Moo-Young [26]. For both low and higher air superficial velocities, the correlation of Hughmark gives the closest predictions. For low air superficial velocities, the correlation of Joshi and Sharma and the correlation of Kawase and Moo-Young well predict the experimental data. The correlation of Reilly et al. gives a similar trend to the experimental data; however a constant shift of volume fraction is noted. The inner pipes may influence the trend of the holdup, thus further investigations without the presence of the inner pipes is required.

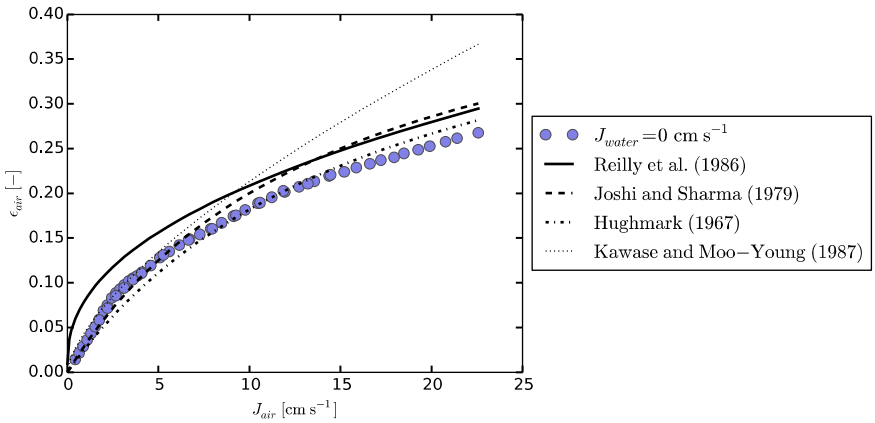

Figure 8. Holdup measurement (J_{water} = 0 cm/s): comparison with literature correlations.

4.3. Optical probe measurements

Three to four measurements were performed at low air superficial velocities while two measurements were taken at moderate and high superficial air velocities. These measurements were performed for the four water superficial velocities investigated in the holdup analysis (figure 9). Four of the six point analysed of the bubble column configuration (J_{water} = 0 cm/s) are the same of flow visualisation previously described (figures 3 to 6). In the following, some comments are outlined.

Concerning the local void fraction (figure 9a), there are three considerations. Firstly, it increases with superficial air velocity, such as expected. Secondly, it increases with superficial water velocity. This is because bubbles move in a non-stagnant surrounding liquid, which is forced to move downward. In a time averaged point of view, this means that the same amount of mass flow for unit of volume needs more time to flow out from a control volume. Therefore void fraction increases. Thirdly, comparing local and global void fraction (figure 10). some consideration on void fraction profiles can be outlined: (i) a negative difference value (gas holdup < local void fraction) may indicate a centre peak void fraction profile; (ii) a zero difference value (gas holdup ≈ local void fraction) may indicate a flat void fraction profile; (iii) a positive difference value (gas holdup > local void fraction) may indicate a wall peak void fraction profile. The global-local void fraction comparison is a matter of further studies.

Concerning the bubble vertical velocity (figure 9b), an increase in air superficial velocity leads to an increase in bubble vertical velocity as one would expect. The increase of the bubble vertical velocity after the transitional superficial gas velocity is due to the increased coalescence rate. The increase in superficial water velocity, which we recall flows downward, also leads to increase in bubble vertical velocity. This indicates that the velocity in the recirculation cells may become higher. Furthermore, liquid may be more concentrated near walls and an increase of liquid velocity may results in the

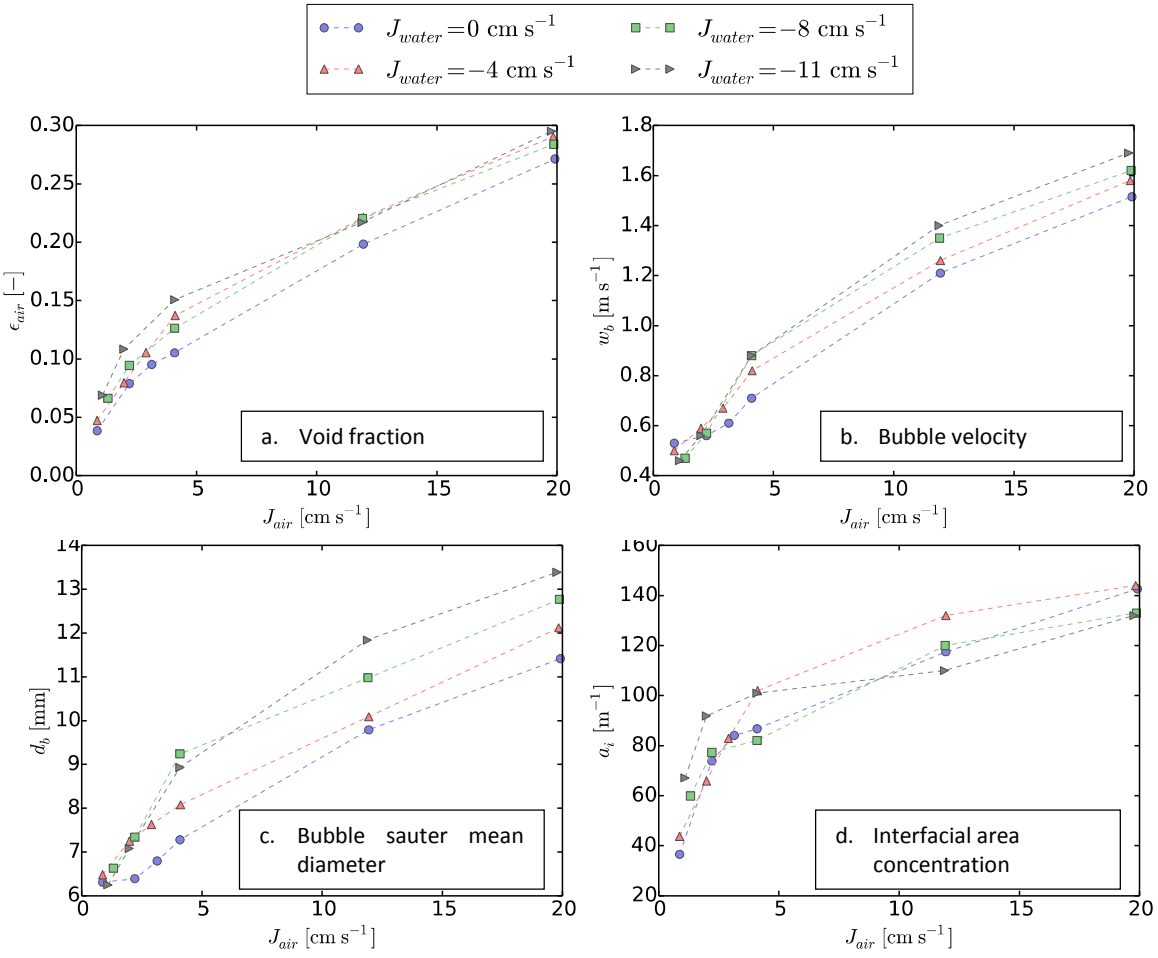

Figure 9. Optical probe measurements.

increase of the thickness of the liquid film near walls. This would result in the increase of the velocity of the gas phase in the core of the section.
Concerning the bubble Sauter mean diameter (figure 9c), it increases with air and water flow rate. The authors think that this trend is caused by the increased turbulence. An increased turbulence would cause an increase in the coalescence rate due to the higher number of collisions. The reasons for this trend can be linked to the coalescence phenomena [27]. It should not escape notice that the sauter mean diameter refers to the hypothesis of spherical shape. In the churn turbulent flow regime it is better to refer to bubble size distribution rather to a bubble Sauter mean diameter. The bubble diameter distribution for the churn turbulent regime is presented in figure 11. It should not escape notice that above distribution is obtained from a chord length distribution and the assumption of spherical bubbles. Above distribution should be corrected taking into account the shape of the bubbles. However, from the above figure some considerations can be outlined. It seems that in the fully developed churn turbulent flow, the peaks of the distributions increases decreasing water flow rate. This suggests that higher liquid flow rate induces a more uniform bubble size distribution.
Concerning the interfacial area concentration (figure 9d), it shows an increasing trend with the increase of water superficial velocity at low air superficial velocity and an opposite trend at higher air superficial velocity. This means that, as the bubble diameter increases, the interfacial area concentration decreases after some point.

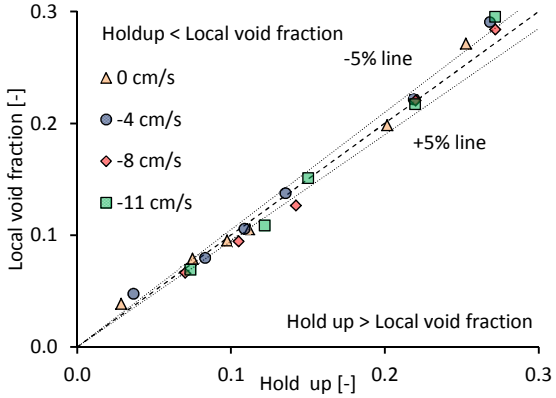

Figure 10. Local and global void fraction comparison. -- lines represent the ±5% difference.

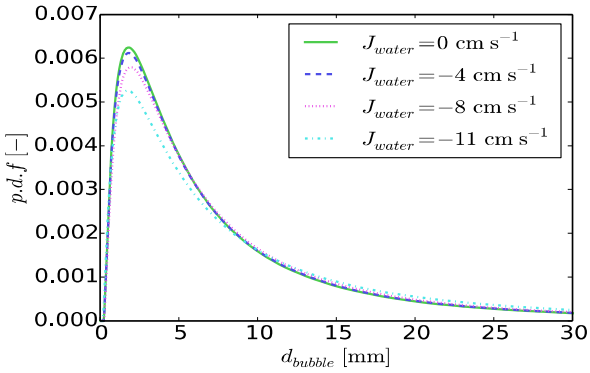

Figure 11. Bubble diameter distributions for the churn turbulent regime.

5. Conclusions

This paper investigates the air-water counter-current flow in a large diameter vertical pipe at ambient temperature and pressure. The inner pipe is 240 mm diameter and has two inner pipes. This layout has never studied in the literature The following range of operating conditions was analysed: superficial air velocities up to 23 cm/s and superficial water velocities up to - 11 cm/s, corresponding to global air volume fractions up to 29%. The experimental investigations concerned (i) flow visualization, (ii) local data from a double fibre optical probe and (iii) holdup data. A homogeneous-bubbly flow regime and a heterogeneous-churn turbulent flow regime have been reported with a transition zone between the two regimes. In the homogeneous regime bubble recirculation occurs around the inner pipes along with the periodic appearance of cap-bubbles. The cap-bubbles seems to originate along the inner pipes because of the coalescence phenomena. Due to the presence of these cap-bubbles this regime can be better defined as a pseudo-homogeneous regime. In the heterogeneous regime periodic very large bubbles which occupy the majority of the cross section of the pipe are observed. The stable slug flow and the annular flow and the flooding condition were not observed. The absence of slug flow is motivated by theoretical consideration on large diameter pipe. The flow regime transition has been analysed using holdup measurements. Flow regime transition between bubbly and transition regime starts at a certain transitional gas velocity, which decrease while increasing the superficial liquid

velocity. In the bubbly flow regime gas holdup increases linearly as a function of the gas flow rate. Moreover, it increases with water flow rate. The transition toward the heterogeneous regime is completed at about $\varepsilon_{air} \approx 16\%$. Above $\varepsilon_{air} \approx 17$ %, the water superficial velocity has no influence on the holdup. Possible explanations for the phenomena are given and discussed. At the present state, the role of inner pipes on flow behaviour is not clear and is a matter of further study. A comparison between holdup measurements and literature correlations has been performed. Local flow behaviour has been analysed considering the local void fraction, the bubble velocity, the bubble diameter and the bubble diameter distribution. Local void fraction, bubble mean diameter and bubbles velocity increase with air and water flow rate, which have been critically analysed and commented. Analysing the bubble diameter distribution in the churn turbulent flow regime, it seems that higher liquid flow rate induces a more uniform bubble size distribution. At certain operating conditions global and local void fraction values are very similar and this may suggest a flat void fraction profile. At other operating conditions the difference may suggest a wall peak or a centre peak void fraction profile. Further studies may concern the influence of the inner pipes of the flow behaviour, a more detailed analysis of the flow regime transition and the study of the local flow behaviour. Finally, it would be interesting to analyse the images for providing data concerning the bubble shape.

References

[1] Yamaguchi K and Y. Yamazaki Y 1982, *J. Nucl. Sci. Technol.***19** 985-96
[2] Hasan A R, Kabir C S and Srinivasan S 1994 *Chem. Eng. Sci.* **49** 2567-74
[3] Aritomi M, Zhou S, Nakajima M, Takeda Y, Mori M and Yoshioka Y 1996 *J. Nucl. Sci. Technol.***33** 915-23
[4] Aritomi M, Zhou S, Nakajima M, Takeda Y and Mori M, 1997 *J. Nucl. Sci. Technol.***34** 783-91
[5] Zhou S, Suzuki Y, Aritomi M, Matsuzaki M, Takeda Y and Mori M 1998 *J. Nucl. Sci. Technol.***35** 335-43
[6] Fuangworawong N, Kikura H, Aritomi M and Komeno T 2007 *Chem. Eng. J.***130** 111-8
[7] Ghosh S, Pratihar D K, Maiti B and Das P K 2012 *Chem. Eng. Sci.* **84** 417-36
[8] Ghosh S, Pratihar D K, Maiti B and Das P K 2013 *Int. J. Multiphas. Flow* **52** 102-20
[9] Kataoka I and Ishii M 1987 *Int. J. Heat Mass Tran.***30** 1927-39
[10] Brooks C S, Paranjape S S, Ozar B, Hibiki T and Ishii M 2012 *Int. J. Heat Fluid Fl.* **37** 196-208
[11] Serizawa A and Kataoka I 1990 *Nucl. Eng. Des.* **122** 1-16
[12] Ohnuki A and Akimoto H, 1998 *Proc. Third International Conference on Multiphase Flow, ICMF '98* (Lyon, France)
[13] Elghobashi S and Abou-Arab T W 1983 *Physics of Fluids* **26** 931-8
[14] Hibiki T and Ishii M 2003 *Int. J. Heat Mass Tran.***46** 1773-90
[15] Ohnuki A and Akimoto H 2000 *Int. J. Multiphas. Flow* **26** 367-86
[16] Schlegel J P, Sawant P, Paranjape S, Ozar B, Hibiki T and Ishii M 2009 *Nucl. Eng. Des.* **239** 2864-74
[17] Al-Oufi F M, Cumming I W and Rielly C D 2010 *Can. J. Chem. Eng.* **88** 482-90
[18] Reilly I, Scott D, Debruijn T and MacIntyre D 1994 *Can. J. Chem. Eng.* **72** 3-12
[19] Barrau E, Rivière N, Poupot C and Cartellier A 1999 *Int. J. Multiphas. Flow* **25** 229-56
[20] Vejražka J, Večeř M, Orvalho S, Sechet P, Ruzicka M C and Cartellier A 2010 *Int. J. Multiphas. Flow* **36** 533-48
[21] Hyndman C L, Larachi F and Guy C 1997 *Chem. Eng. Sci.* **52** 63-77
[22] Krishna R, Wilkinson P M and Van Dierendonck L L 1991 *Chem. Eng. Sci.* **46** 2491-6
[23] Reilly I, Scott D, De Bruijn T, Jain A and J. Piskorz 1986 *Can. J. Chem. Eng.* **64** 705-17
[24] Joshi J and Sharma M 1979 *Chem. Eng. Resw. Des.***57** 244-51
[25] Hughmark G A, 1967 *Ind. Eng. Chem. Proc. DD.* **6** 218-20
[26] Kawase Y and Moo-Young M 1987 *Ind. Eng. Chem. Res.* **26** 933-7
[27] Oguz H N and Prosperetti A 1993 *J. Fluid. Mech.* **257** 111-45